This article has been accepted for publication in a future issue of this journal, but has not been fully edited. Content may change prior to final publication. Citation information: DOI 10.1109/ACCESS.2020.3017888, IEEE Access

IEEE Access
Multidisciplinary | Rapid Review | Open Access Journal

Date of publication xxxx 00, 0000, date of current version xxxx 00, 0000.

Digital Object Identifier 10.1109/ACCESS.2017.DOI

An effective zeros-time windowing strategy to detect sensorimotor rhythms related to motor imagery EEG signals.

Kais Belwafi[1], Sofien Gannouni[1], and Hatim Aboalsamh [1]
[1]Department of Computer Science, College of Computer and Information Sciences, King Saud University, Riyadh, KSA.

Corresponding author: Kais Belwafi (e-mail: kbelwafi@ksu.edu.sa).

The authors extend their appreciation to the Deanship of Scientific Research at King Saud University for funding this work through Research Group no. RG-1440-109.

ABSTRACT

Brain-computer interface (BCI) acquires, analyzes and transforms human brain activity to control commands allowing as such disabled people to communicate or control external devices. A motor imagery-based BCI enables patients to control artificial peripherals and communicate with the outside world by merely thinking of the task such as, e.g., the imagination of left-hand, right-hand, or foot movement. The mere intention of moving one of the limbs triggers neural activity, which is induced in the primary sensorimotor areas like that observed with real executed movements. Tracking generated sensorimotor rhythms (SMRs) and extracting robust and informative features from electroencephalogram (EEG) signals are challenging due to the time-varying nature of EEG signals and the inter-human variability. In this paper, we proposed an EEG-zeros-time windowing (E2ZTW) approach based on a highly decaying window function to track SMRs and identify the temporal epochs containing useful information without any prior information on the trigger. The proposed approach involves the application of the group-delay function, allowing the improvement of the spectral resolution due to the additive property of the function on individual resonances. Some algorithms were integrated into the proposed approach, such as the common spatial pattern algorithm, which is used to extract features and linear discriminant analysis and a convolutional neural network, which are used for the classification of the features. The effectiveness of the proposed approach in tracking the SMRs rhythms is evaluated in terms of accuracy. Experiments were performed on three public datasets provided by BCI competition for 17 subjects. Following experimental results, it is shown that discrimination between the left- and right-hand movements can be achieved within a few seconds with high classification accuracy. As compared to other state-of-art techniques, the proposed approach achieves an average classification accuracy and standard error values of 82% and 13, respectively, thereby outperforming existing algorithm by an accuracy mean of 2%.

INDEX TERMS Brain-computer interface (BCI), electroencephalography (EEG), motor imagery, EEG-Zero-time windowing, Group-delay function

I. INTRODUCTION

In recent years, the advancement in technology, as well as information technologies, has provided an improved understanding of the brain's response to physical phenomena; this has made it possible to design a brain–computer interface (BCI) system for functional substitution or pathological analysis [1], [2]. No matter what the application is, the electroencephalogram (EEG) signal processing chain remains the same and includes three progressive processing stages: EEG filtering, feature extraction, and classification, as shown in Figure 1. The main difference between these application domains is the feedback, which is sent to an artificial agents in the field of functional substitution and a practitioner for pathological analysis. The performance of signal decoding is a key precondition for effective BCI applications [3]. Classification results are used to control artificial agents or are converted into useful presentations for the practitioner.

EEG changes can be categorized into two main categories:

This work is licensed under a Creative Commons Attribution 4.0 License. For more information, see https://creativecommons.org/licenses/by/4.0/.

This article has been accepted for publication in a future issue of this journal, but has not been fully edited. Content may change prior to final publication. Citation information: DOI 10.1109/ACCESS.2020.3017888, IEEE Access

event-related potentials (ERPs) and spontaneous signals. ERPs such as SSVEPs (steady state visual evoked potentials) and P300 are usually defined in the time domain as brain electrical activity that is arising in reaction to external particular events or stimuli [4], [5]. Spontaneous signals are defined in time and frequency domains as brain activity that is triggered independently from external events. They are directly and consciously triggered by the user by muscular contractions or by thinking about specific tasks [6]. The scope of this paper is the use of spontaneous signals known as EEG motor imagery (MI) signals for functional substitution applications.

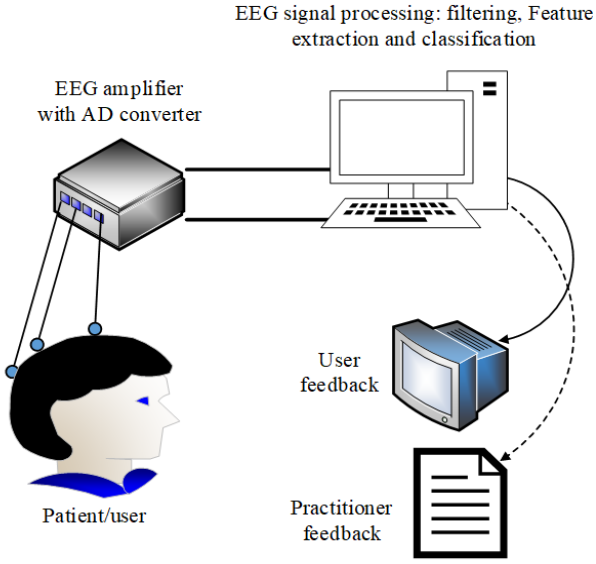

FIGURE 1: Typical EEG signal processing chain

During brain activity, while moving one of the human's limbs, the shape of SMRs changes continuously with time. Evoked SMRs appear and vary continuously in specific frequency bands such as (α, [8-12] Hz), (β, [8-30] Hz) and (γ, [30-60] Hz) [7], [8]. Furthermore, these rhythms appear at a specific location of the brain lobes, depending on the limbs moved. Hence, any study on brain activity should take into account temporal, spectrum, and spatial features. From this point of view, it is difficult to extract features of the changing SMRs from the EEG signals.

Generally, most attempts to decode MI signals, especially through synchronous approach, used a fixed time window starting at 0.5s before the cue and lasted for 2s to 4s [9]–[12]. However, a fixed time window approach corrupts the information in the frequency domain by adding irrelevant information. Also, using a fixed time window approach is not always effective, as this approach assumes that a subject will start thinking about the MI task immediately after the cue appears [13]. This approach commonly leads to low classification accuracy because of interference from invalid data [14]. Following the above shortcomings in using a fixed window, an effective and accurate approach would be to track SMRs while using short-time intervals, which can adequately represent the state of subjects and avoid stationarity problems [15]. Furthermore, using the short-time window approach improves the accuracy of brain activity classification while reducing computational resources.

Concerning the frequency bands, always a fixed bandwidth is used to cover α and β bands whatever containing a significant statistical information or no. It is worthy to notice that the same frequency band cannot be defined for two or more users due to the intrinsic variability between subjects [10], [16]. Furthermore, the SMRs rhythms is highly dependent to subject health status of subjects or the environment [17]. A feasible architecture is, therefore, required for the automatic selection of active spectra susceptible to contain useful information for each subject. The last factor, which is the spatial location of the electrodes, is essential and should be taken into account during brain activity discrimination. SMRs appear in a specific location of the brain when there is an intention to move one of the human limbs [18], [19].

In [20], Jing et al., proposed a new filter approach based on correlation analysis to reduce the number of EEG channels used during the recording process by removing channels which are relatively uncorrelated with one another across trials. The proposed correlation-based channel selection method allows to reach an average classification accuracy of 85% versus 72% compared to the algorithm using all channels. The presented method selects only the relevant channels without studying the effect of the time window. A correlation-based time window selection (CTWS) algorithm for MI-based BCIs is proposed to localize the epoch containing the MI-EEG signals for each trial in all subjects [14]. The CTWS approach is based mainly on the identification of reference signals (R) for each class label and localize the time window of each trial having the maximum correction with R. The proposed system used CTWS, CSP and SVM and has been validated according to the offline approach on 7 subjects. The average accuracy was 77.3%. The identification of the reference signals (R) remains the main disadvantage of such approach and should be well done during the training process and updated even during the test process. In [21], Patcharin et al., proposed a deep learning approach with a joint training scheme to recognize and track the pure imagery and non-pure imagery EEG signals. A channel selection is peformed manually by selecting only three electrodes C_3, C_z and C_4 allowing to reach a mean classification accuracy beyond 71% and 70% using, respectively, the CNN-FC and the CSP with SVM algorithms. In [22], Rattanaphon et al., investigated the role of action observation and MI during the standing and sitting tasks. In this study, a fixed time window of 2s with an overlapping factor of 0.2s and 9 filter banks are used to track EEG rhythms during the sit-to-stand and stand-to-sit transitions. The average accuracy obtained with the filter bank common spatial pattern (FBCSP) and SVM is about 82%. The tracking of the EEG SMRs rhythms is time-consuming due mainly to the preprocessing block containing many time windows and nine filter banks.

In this study, we propose a novel EEG-zeros-time window-

This work is licensed under a Creative Commons Attribution 4.0 License. For more information, see https://creativecommons.org/licenses/by/4.0/.

This article has been accepted for publication in a future issue of this journal, but has not been fully edited. Content may change prior to final publication. Citation information: DOI 10.1109/ACCESS.2020.3017888, IEEE Access

ing (E2ZTW) algorithm for MI-based BCIs system. First, all the trials (T) of training and testing sessions are segmented into N_w frames (F_w) containing F_l samples. This step involves the multiplication of a short segment of the EEG trial with a filter window resulting in an impulse-like signal with most of the energy at the beginning of the frame. Second, a group-delay function is used to compute and extract the EEG spectra with high-resolution in order to automatically identify the F_w containing the active spectral characteristics of the trial. These steps allow selecting the useful part of EEG signals from long (effectively much more than 7 seconds) brain trial segments. Third, the group-delay function were used to tract and identify the most active SMRs rhythms comprised between 0Hz and $\frac{Fs}{2}$Hz for both training and testing samples. Fourth, the E2ZTW method integrate a process based-on voting technique allows to select the channels that contained more correlated information to improve the classification performance of MI-based BCIs. Finally, the proposed system integrates the common spatial pattern (CSP) as a feature extraction technique and both linear discriminant analysis (LDA) and convolutional neural network (CNN) to classify the features. Two EEG recording sessions are used to evaluate the system performance where one session is used for training and the other for test.

The rest of this paper is organized as follows. Section II describes the terminology and annotations used in this paper. Section III introduces real EEG data used for evaluation and discusses the basis of the proposed method for deriving spectral EEG information from different trials related to left- and right-hand movements. Also, the section discusses the effect of the analysis window to track SMRs and identify the relevant EEG channels used during the recording process. This is followed by comparison results and discussions in Section IV. Finally, the conclusion is given in Section V.

II. TERMINOLOGY AND ANNOTATIONS

- For each subject (s) from a set of subjects (S), a set of trials (T) is recorded.
- A channel (c) is used to record EEG signals from the scalp.
- C is a set of channels used during the recording.
- Fs is the frequency sampling of the EEG recording.
- e is a sample of trial.
- E is a set samples e of each trial t.
- $t(E, C)$ is a trial with dimension E samples and C channels.
- E_{og} is EoG channels used to record ocular artifacts during the recording of each trial (t).
- F_w is a frame window of trial t with length F_l samples.
- F_a is an appended frame windows.
- ϱ is the appending operator.
- O represents the overlap between two successive window;
- χ_t represents the discrete Fourier transform (DFT) of a trial t. It is a complex value ($\Re$+j$\Im$).

III. METHODS AND MATERIALS

A. BENCHMARKS DATASET

In this study, experiments are conducted on three datasets from a BCI competition containing EEG recording for 17 subjects. The recording contains cued MI (multi-class) with 4 classes related to the left hand, right hand, both foot, and tongue. Details about these datasets can be found in [23]–[25]. The common link between these datasets is the timing paradigm of the trials, which is shown in figure 3. Each of the experiments consisted of two sessions with at least 240 trials in each session; Two seconds after each trial had started were quiet, and then, an acoustic beep was heard indicating the beginning of the trial. At the end of each trial, a cross symbol "+" was displayed, and 3s after this, an arrow to the left, right, up, or down was displayed for 1s; at the same time each subject was respectively asked to imagine moving his/her left hand, right hand, tongue, or foot, and this lasted for 7s until the cross symbol disappeared.

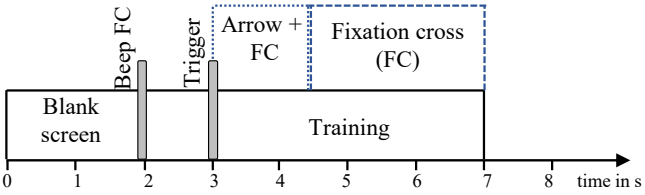

FIGURE 2: Timing of the recording of the EEG trials (T) [25].

B. EEG-ZERO-TIME WINDOWING

1) Basis for the proposed method

An EEG-zero-time windowing (E2ZTW) approach is proposed to extract the spectral characteristics from very short segment of the EEG trials. The E2ZTW approach involves multiplying a short duration of each trial at each channel with a window function similar in shape to the frequency response of zero-frequency resonator [26]. The window function is given by:

$$\psi[n] = \begin{cases} 0, & n = 0 \\ \frac{1}{4sin^2(\frac{\pi n}{2N})}, & n = 1, 2, ..., F_l - 1 \end{cases}$$

where F_l is the window length. The first value of the window $\psi[0]$ is initialized to zero to avoid division by zero error and make the mean value of the windowed signal spectrum to be zero without altering the spectral peaks. Such a window function ψ does not stop the discontinuities of the signal abruptness in the time domain unlike any other window function [27]. In this study, we used two spectrum extractions techniques: the discrete Fourier transform (DFT) denoted by χ and the group-delay function. The group-delay function was used to extract spectra with high-resolution properties and highlight the formant features of the spectra. The group-delay function was computed according to the following equation (Eq 1):

This work is licensed under a Creative Commons Attribution 4.0 License. For more information, see https://creativecommons.org/licenses/by/4.0/.

This article has been accepted for publication in a future issue of this journal, but has not been fully edited. Content may change prior to final publication. Citation information: DOI 10.1109/ACCESS.2020.3017888, IEEE Access

$$\varphi(t,c) = \frac{\Re(\chi_t(c))\Re(\chi_{t_n}(c)) + \Im(\chi_t(c))\Im(\chi_{t_n}(c))}{\Re(\chi_t(c))^2 + \Im(\chi_t(c))^2} \quad (1)$$

where $t_n(n,c) = nt(n,c)$. We report that division by the square of the magnitude in the θ and γ bands can lead to problems due to small brain activities during MI. The division by the squared magnitude, in this case, can be completely avoided, and only the numerator of the group-delay (NGD) function is used.

During the recording of the BCI competition EEG datasets, subjects performed MI once the cue appeared for 4s, as depicted in Figure 2. Winners of the BCI competition and several related research studies considered only the first 2s starting at 0.5s after the cue [9]–[11]. Assuming that this assumption is true, in the first part of this study, we considered the same segment of the EEG trials starting at 0.5s to 2.5s after the cue, as shown in Figure 3(a). The windowed EEG signals obtained by applying the window function ψ once (one time) and twice (two times) are shown in Figure 3(b) and 3(c). Figures 3(d), 3(e), and 3(f) show the spectrum of the EEG segments in Figure 3(a), 3(b) and 3(c), respectively. Applying the window ψ results to an impulse-like signal with most of the energy at the start of the window, as shown in Figure 3(b). Furthermore, more attention was given to the EEG signals at the start of the window. This was necessary if the objective was to obtain brain activity response characteristics at important events during MI, such as at moments of significant excitation of the brain, when the intention was to move the left or right hands. Figure 3(g), 3(h), and 3(i) illustrate respectively the NGD plots of the signals in Figure 3(a), 3(b), and 3(c). The spectral features can be better seen in Figures 3(g) and 3(h) as compared respectively to Figures 3(d) and 3(e), especially the obtained spectra in the α and β bands that are likely to contain the useful information about the MI signals. So, as shown in Figure 3, the main advantages of the used windowing function is that it maintains the most energy at the beginning of the frame. Applying the time window more than one time leads to an impulse like Dirac delta function, as mentioned in Figure 3(c), and it will be very hard to analyze the frequency components as depicted in Figure 3(f). So, applying the window function more than one time is not suitable in the analysis of MI EEG signals. However, applying the time window two successive times or more can be useful in the analysis of EEG signals having a high sampling frequency.

2) Zero-time windowing approach for instantaneous spectral features of an EEG trial

Algorithm 1 illustrates the basic steps of the E2ZTW approach. For each dataset, trial, and channel, the EEG samples were windowed by ψ, with length F_l, after appending the signal by $(Fs - F_l)$ zeros to set its length to Fs. To track the SMRs in each epoch of 0.5s corresponding to $\frac{Fs}{2}$ samples, the window length F_l was initialized to 0.5s. It is worthy of note that consideration should be given to the overlap factor O, where the frame F_l exceeds the Fs to capture the abrupt changes in the SMRs. Each analysis segment was appended in this case with $\frac{Fs}{2}$ zeros. Subsequently, the NGDs at each channel and each trial are computed according to equation (Eq1).

Algorithm 1: Commented algorithm of basic steps of E2ZTW in Matlab

Data: $t(E,C)$
Result: NGD of t (t_{NGD})
$F_l = 0.5$;
$O = 0$;
$S_t = (1-O) * F_l$ *// Starting point of the next frame* ;
$N_w = floor((E/Fs - F_l)/S_t)$ *// Number of the frame window per trial* ;
for *c=1:C* **do**
  for $t = 1{:}T$ **do**
    for $n_w = 1{:}N_w$ **do**
      $temp = floor((n_w - 1) * S_t * Fs + 1))$;
      F_w=$t(temp : temp+(F_l * Fs), c) * \psi(Fs)$;
      if $F_l * Fs \leq Fs$ **then**
        $F_a = \varrho(F_w, Fs)$;
        else
          $F_a = F_w$;
      $n = 1$ {1,2, .., Fs };
      $y_w = n * F_a$;
      [T_{wR}, T_{wI}]=$\chi(F_a$,$Fs)$;
      [Y_{wR}, Y_{wI}]=$\chi(y_w$,$Fs)$;
      $k = 1$ {1,2, .., $\frac{Fs}{2}$ };
      $t_{NGD}[k] =$
       $T_{wR}[k]Y_{wR}[k] + T_{wI}[k]Y_{wI}[k]$;

In this subsection, the overall samples of each trial were taken into consideration. Figure 4(a) shows an example of a trial captured through the electrode c_3 located in the parietal brain lobe. The main advantage of considering the overall trial length was to study the brain activity before and after the appearance of SMRs that was evoked when a subject thinks of moving one of his hands. The NGD and the DFT spectrum plots obtained at every sampling instant are shown respectively in Figures 4(b) and 4(c). Both plots are scaled to 40 points, corresponding to the frequency range of 0 to 40 Hz; they are susceptible to contain MI signals. Figure 4 shows that the E2ZTW approach enhances the appearance of the temporal resolution of the spectral feature. Concerning the NGD and the DFT spectrum plots, as shown in Figure 4(b), the SMR signals are observed better than the standard DFT spectrum plots. Furthermore, it can be visually interpreted from Figure 4(b) that the SMR signals appeared in the 2^{nd} to 8^{th} time window in the studied trial, which is 0.5s to4 s from the trial recording. Conversely, from the DFT spectrum representation in figure 4(c), it is difficult to localize the time window containing SMRs or useful information. The windowed signals has approximately the same reliefs, except

This work is licensed under a Creative Commons Attribution 4.0 License. For more information, see https://creativecommons.org/licenses/by/4.0/.

This article has been accepted for publication in a future issue of this journal, but has not been fully edited. Content may change prior to final publication. Citation information: DOI 10.1109/ACCESS.2020.3017888, IEEE Access

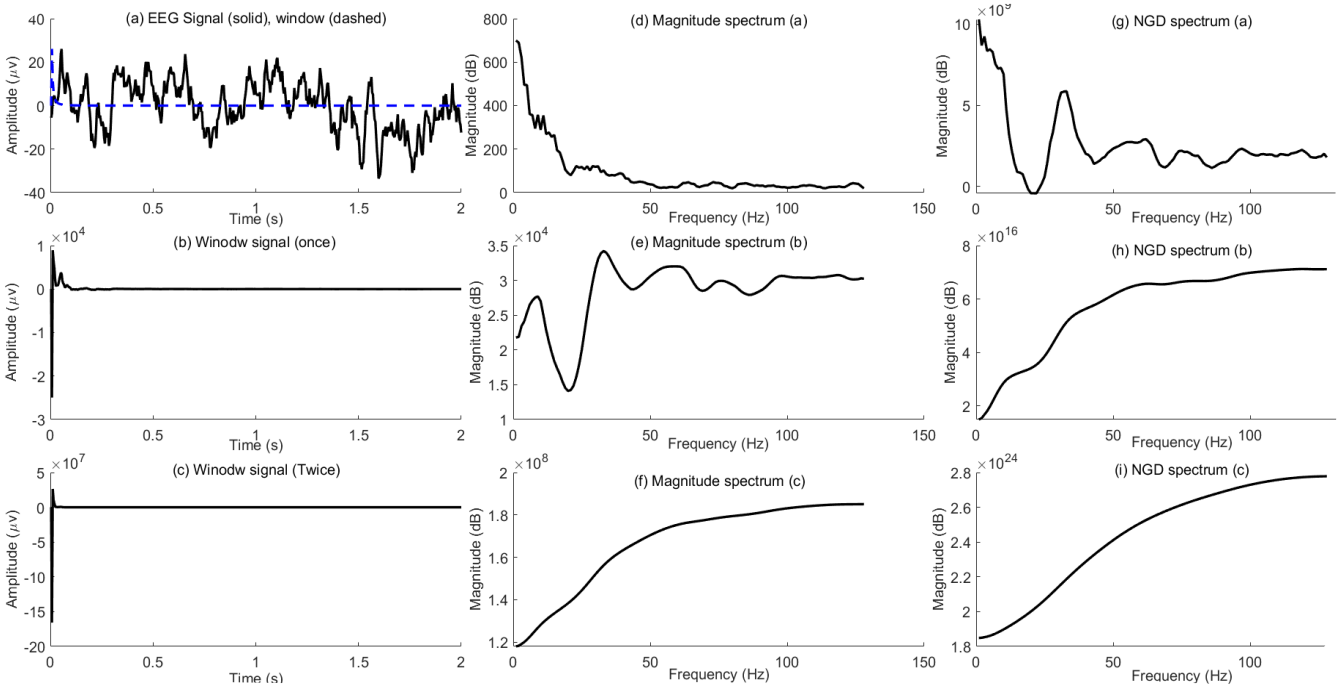

FIGURE 3: Illustration of E2ZTW and DFT spectrum for a short segment (0.5 s) of EEG trial.

the 3^{rd} time window.

C. EFFECT OF WINDOW SIZE

The main parameter of the instantaneous feature extraction methods is the ψ window size. It has a direct effect on the recognition of trials and the required trial classification time. The smaller and more defined the window size, the smaller the classification error rate and the lesser the number of processing samples, allowing the processor to offload its task. To examine in detail the effect of the window size and track a subject's intended movement, a different window size was applied to the EEG signals corresponding to 0.25s and 0.125s. Figure 5 shows the NGD and the squared magnitude spectrum plots of the EEG signal $t(E, c3)$; which is depicted in Figure 4(a). The plots show that the SMRs are obtained for small window size and appeared at the same time interval. As shown in Figure 5, a decrease in the window size is accompanied by the highest of the spectral peaks and the lowest of the frequency resolution. Conversely, the ripple as a result of truncation can be seen in the NGD plots due to the smaller period of the EEG signals in the frequency domain.

D. ANALYSIS OF DIFFERENT CATEGORIES OF TRIALS

In this subsection, we will use the proposed E2ZTW approach to analyze the spectral features for two trials (t_r and t_l corresponding respectively to right- and left-hand intentions). The analysis is focused on channels c_3 and c_4, which are susceptible to contain the SMRs related to the hands' intended movements [18], [25]. Furthermore, the time window size ψ is set to 0.5s throughout this analysis. The instantaneous spectral features are displayed using the NGD function of the windowed data due to the effectiveness in tracking the SMRs, as described in the previous sections. Figure 6 shows the temporal variation and NGD plots of two trials (t_r and t_l) corresponding to left- and right-hand intentions at c_3 and c_4 channels. To analyze these variations, it is critical to consider, from a neuroscience viewpoint, the montage used during the recording process shown in Figure 7. When there is an intention to move the right hand (respectively the left hand), SMRs should be shown at the electrode c_3 (respectively at the electrode c_4). As shown in figure 6, at the electrode c_3 and after the 6^{th} window, the SMRs are completely dissimilar, except for some time window epochs. Interestingly, the NGD plots show the event-related desynchronization (ERD) of the intention to move the right hand where the magnitude is significantly reduced compared to SMRs at the same electrodes for the intention to move the right hand. Also, It is worthy of note that ERD/ERS appeared without considering the rest period, as computed in [28]. The SMRs are also shown for the trials at the electrodes c_4, except for some window epochs. This last dilemma remains the most delicate task, and these time window epochs should not be considered when instantaneous features are extracted.

E. SMRS RHYTHMS TRACKING

The spectral characteristics of trials T are distinct, that is, SMRs change continuously in both time and frequency. These variations are mainly due to the neurophysiology state of subjects, which vary not only form one subject to another but also vary from time to time for the same subject [15].

This work is licensed under a Creative Commons Attribution 4.0 License. For more information, see https://creativecommons.org/licenses/by/4.0/.

This article has been accepted for publication in a future issue of this journal, but has not been fully edited. Content may change prior to final publication. Citation information: DOI 10.1109/ACCESS.2020.3017888, IEEE Access

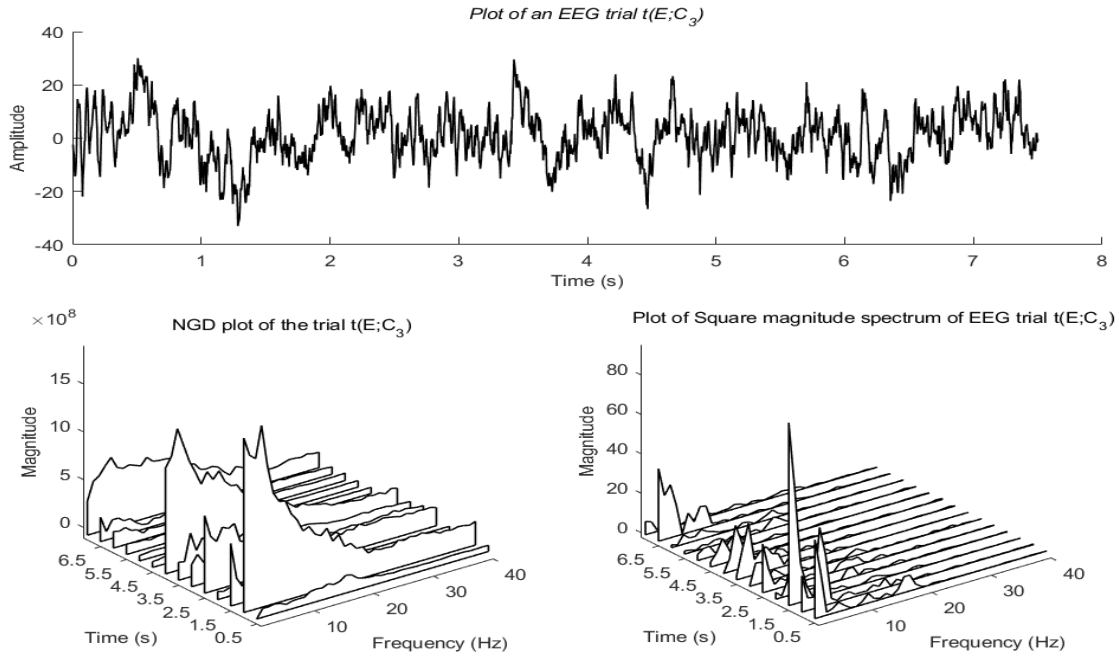

FIGURE 4: NGD and DFT spectrum for a short segment (0.5s) of a trial at channel C_3.

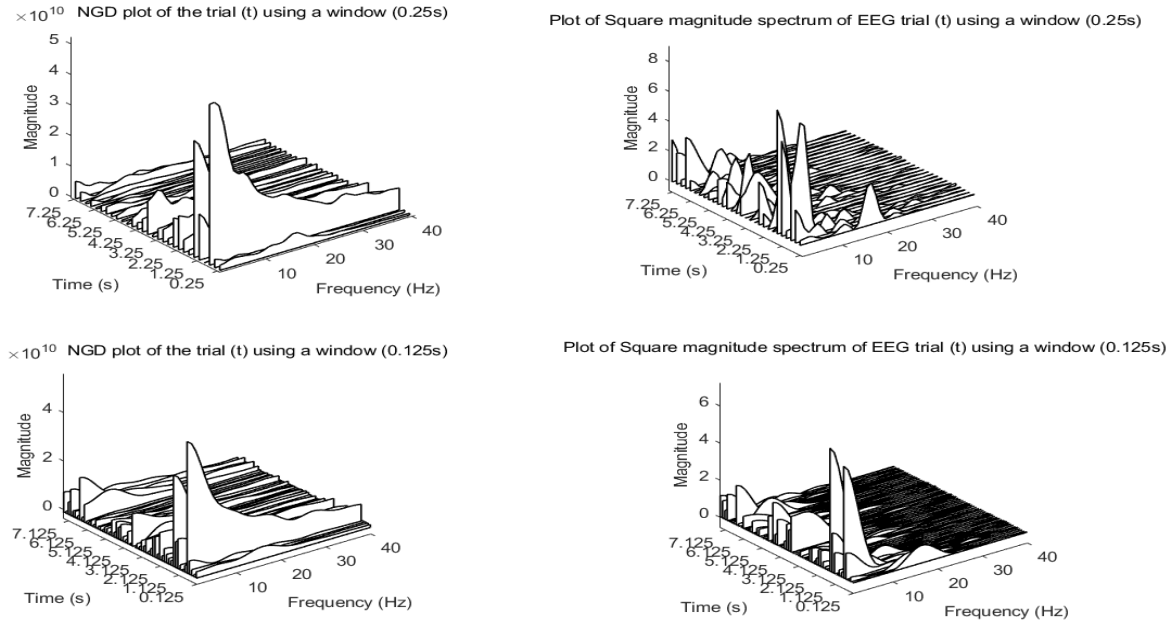

FIGURE 5: Illustrations of the effect of the window size on the the NGD and DFT spectrum.

Thus, identifying the pertinent information related to MI intention remains a key factor to develop a high-accurate BCI chain. In this regard, based on the presentation of the NGD plots, we proposed a method to study the area under curve (AUC) of each window to track the high variation in time and frequency. Algorithm 2 presents the basic steps of the proposed method to select the appropriate window based on the analysis of the AUC of each time window in the band $[f_{min} f_{max}]$ Hz. The main concept of the proposed method is to localize the window with the maximum variation of the preceding window. This way, the appropriate window at each channel can be localized, and then, a majority voting technique is applied to select the index of the time window that seems to contain the pertinent SMRs. It is critical to note that the proposed method can also select channels containing useful information for each subject; it is essential to reduce

This work is licensed under a Creative Commons Attribution 4.0 License. For more information, see https://creativecommons.org/licenses/by/4.0/.

This article has been accepted for publication in a future issue of this journal, but has not been fully edited. Content may change prior to final publication. Citation information: DOI 10.1109/ACCESS.2020.3017888, IEEE Access

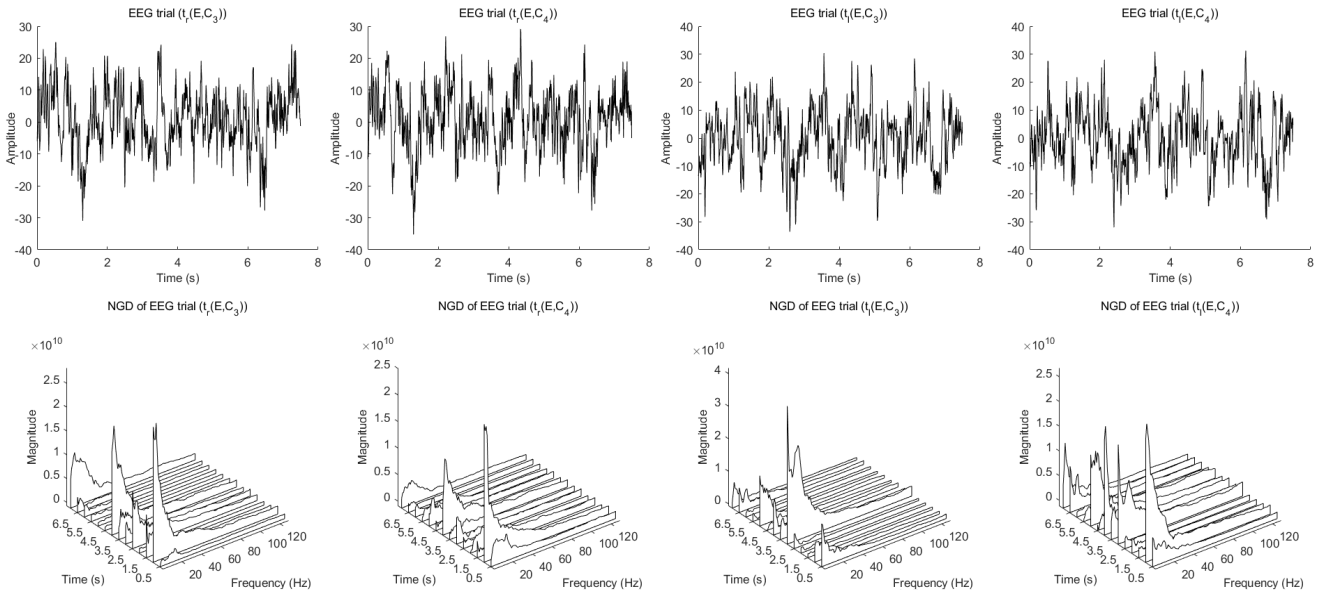

FIGURE 6: Instantaneous NGD spectrum of two trials (left- and right-hand) using a window of 0.5s.

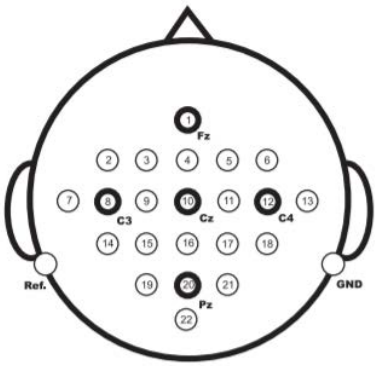

FIGURE 7: Electrode montage corresponding to the international 10-20 system [9]

Algorithm 2: Tracking of the SMRs rhythms

Data: NGD of t: 3D
Result: Index $Index\_W$ and $Index\_C$ corresponding to pertinent EEG windows and EEG channels respectively
for $n_w = 2{:}N_w$ **do**
  for $c = 1{:}C$ **do**
    $Surf(n_w, c)$= $\int_{f_{min}}^{f_{max}} t_{NGD}(f, nw, c)df$ - $\int_{f_{min}}^{f_{max}} t_{NGD}(f, nw-1, c)df$; */* Compute the variation under the curve of each window. */* ;
  end
end
$temp = max(Surf)$; */* Return the index of the curve with the maximum variation. */*;
$Index\_W = vote(temp)$; */* Use majority voting to select the pertinent window index. */*;
$Index\_C = (temp == Index\_W)$; */* Return the index of channel having an active SMRs.*/*

the number of channels and keep the useful channels, accelerating the trial identification process.

F. FEATURE EXTRACTION AND CLASSIFICATION OF EEG TRIALS

To verify that the EEG time window and the identified channels obtained from the algorithm 2 correspond to left- and right-hand intention movements, filter, feature extraction, and classification blocks are included based on the typical BCI chain.The EEG signals at each channel were band-pass filtered using the 5^{th} Butterworth filter. The optimization of feature extraction and classification algorithms is also one of the key points to develop an improved MI system. These algorithms are well studied in the literature compared to the preprocessing of the EEG signals in [29]. Since this study focuses mainly on the problem of tracking the SMRs in EEG signals, we used the common spatial pattern (CSP) algorithm to extract features and two different classifiers linear discriminant analysis (LDA) and a convolutional neural network (CNN) to classify the features. Concerning the feature extraction block, we used the CSP, which is one of the most effective and commonly used transformation technique, to extract ERD/ERS related to MI [30]. The CSP algorithm allows the maximization of the variance between the two classes, i.e., for example, the variance between right- and left-hand MI signals. LDA is arguably the most popular algorithm for MI classification in BCI applications, since it has a relatively low computational requirement and usually provides

This work is licensed under a Creative Commons Attribution 4.0 License. For more information, see https://creativecommons.org/licenses/by/4.0/.

This article has been accepted for publication in a future issue of this journal, but has not been fully edited. Content may change prior to final publication. Citation information: DOI 10.1109/ACCESS.2020.3017888, IEEE Access

good classification results [9]. On the other hand, the CNN is used because it is new and has made impressive advances in feature extraction and MI trial recognitions [31]. Furthermore, CNNs are a class of machine learning algorithms that can make predictions and perform dimensionality reduction. The key difference between CNNs and LDA is that deep learning (DL) models, such as CNNs, have higher learning capacity and are much more flexible. Matlab DL toolbox is used to build the CNN architecture known as ResNet with 1,000 layers, where the last three layers of the network are fully connected. Figure 8 exhibits the whole process of the proposed approach including the internal architectures of E2ZTW, CNN and LDA.

IV. RESULTS AND DISCUSSION

In this section, we discuss the effectiveness of the proposed method in extracting instantaneous spectral features corresponding to the intention to move the left- or right-hand. In previous sections, the aim of the proposed approach is discussed using the NGD plots, where the apparition of SMRs for the subject's intention is shown. Also, these SMRs appeared in different time window slots. Furthermore, it has been shown that some channels used during the recording process do not show any brain activity in the studied bands. Thus, the identified time window slots with the relevant channels should be used to obtain useful information that is likely to contain the SMRs. To evaluate the performance of the proposed method and for comparison purposes, a standard EEG signal processing chain is used. It includes the CSP method as a feature extraction block, and LDA and a CNN as classification algorithms. The EEG signal processing chain is evaluated and validated on three benchmarks proposed by the BCI competition. We state that each dataset contains two recording sessions, where one is used for training and tuning and the other one is used for validation.

Table 1 presents the classification accuracies obtained by the two classifiers (CNN and LDA) according to different E2ZTW parameters. As shown in Table 1, the classification accuracies are too sensitive to the E2ZTW parameters and differ for different subjects. For example, the classification obtained by LDA for subject $s1$ decreases by 20% when using a time window size of 1.75s instead of 1.5s. Maintaining the same configuration for subject $s2$, the classification accuracy is enhanced by 6%. Accordingly, these interpretations confirm that the time window size should be tuned (adjusted) carefully for subjects, mainly due to the inter-subject variability and the subject's reactions to the timing scheme depicted in Figure 2. For the different configurations, LDA outperforms the CNN, where the average classification accuracy exceeds 17% as for the subject $s1$ using the window size ($F_w = 1.5$) and the overlapping factor ($O = 0.25$). This last configuration allows the maximum average accuracy for the three datasets to be obtained. The accuracy gaps between LDA and CNN is due mainly to the small dimension of the extracted features by the CSP. In fact, the CNN model will overfit and provides a bad performance when using small

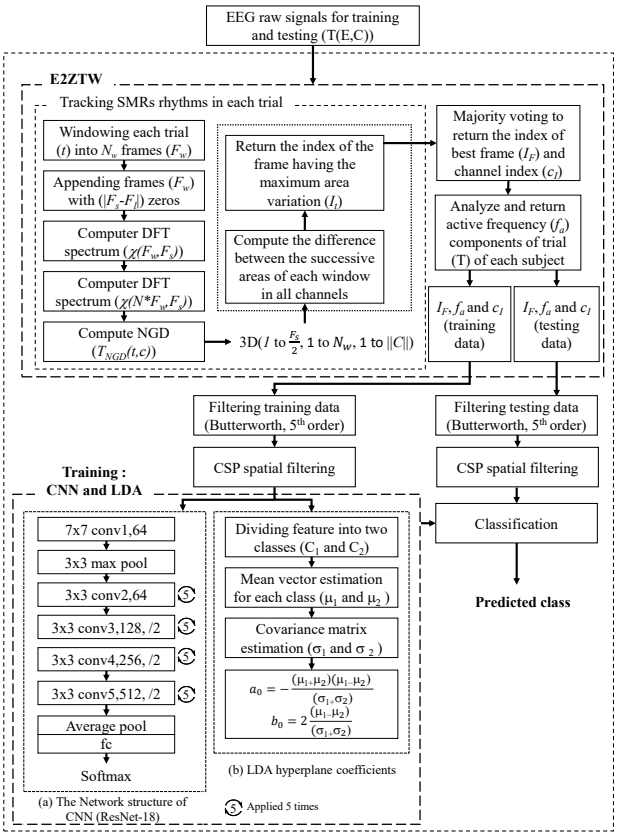

FIGURE 8: Illustration of the proposed approach based on E2ZTW method.

number of features [31]. Unlike CNN, the LDA algorithm outperforms when the dimension of the features per trial is too small and the performance deteriorates significantly when the dimension of the input is increasing [32].

Table 2a shows various metrics including the true positive rate (TP), the true negative rate (TN), the false positive rate (FP), the false negative rate (FN), the precision (Pr), the negative predictive value (NPv), the specificity and the sensitivity that were measured according to the confusion matrix as shown in Table 2b. In fact, Table 2b shows the performance of the proposed method using the LDA classifier, the CSP a feature extraction algorithm and the E2ZTW approach with the best identified parameter ($F_w = 1.5$; $O = 0.25$). The average precision, negative predictive rate, sensitivity and specificity of the proposed method attained 85.30%, 81.85%, 84.86% and 79.17% respectively.

Table 3 presents the accuracy obtained by the proposed method and the overall results of existing methods, which are validated on the same public datasets. The proposed approach significantly improves system performance, achieving an average system accuracy of 82.32%. The effective performance of the E2ZTW approach reflects success for tracking SMRs and localizing time window sizes despite the disuse of trigger information. Furthermore, the results obtained encourage the use of the proposed approach even in asynchronous BCI

This work is licensed under a Creative Commons Attribution 4.0 License. For more information, see https://creativecommons.org/licenses/by/4.0/.

This article has been accepted for publication in a future issue of this journal, but has not been fully edited. Content may change prior to final publication. Citation information: DOI 10.1109/ACCESS.2020.3017888, IEEE Access

$s \in S$	$F_w = 0.25; O = 0$		$F_w = 1.5; O = 0$		$F_w = 1.75; O = 0$		$F_w = 2; O = 0$		$F_w = 1.5; O = 0.5$		$F_w = 1.5; O = 0.25$	
	LDA	CNN	LDA	CNN	LDA	CNN	LDA	CNN	LDA	CNN	LDA	CNN
s1	56.94	56.94	84.72	81.94	69.44	65.27	78.74	74.30	61.80	61.11	87.50	70.83
s2	47.91	47.91	60.41	53.47	59.02	61.80	52.77	51.38	73.61	69.44	75.69	68.75
s3	54.86	52.77	89.58	84.72	82.63	78.47	88.19	81.25	77.08	73.61	93.75	88.19
s4	55.55	51.38	68.05	53.47	52.08	52.08	65.27	63.19	60.41	58.33	58.3	60.41
s5	54.16	54.16	55.55	56.94	56.94	50	55.55	47.91	58.33	57.63	72.91	71.52
s6	50.69	53.47	65.27	63.88	52.08	51.38	69.44	63.19	55.55	60.41	71.52	65.97
s7	43.75	44.44	63.88	76.38	58.33	60.41	56.94	53.47	59.72	55.55	85.41	82.63
s8	54.16	52.08	92.36	91.66	90.27	80.55	86.80	74.72	88.19	82.63	96.52	92.36
s9	56.25	50	84.02	86.80	73.61	66.66	66.66	72.22	70.13	66.66	88.88	84.02
s1	48.88	53.33	83.33	82.22	97.77	95.55	96.66	97.77	48.88	41.11	97.77	87.77
s2	46.66	41.11	61.66	51.66	58.33	53.33	71.66	60	46.66	53.33	73.33	50
s3	66.67	64.44	93.33	83.33	96.66	98.33	91.66	81.66	53.33	50	93.33	80
s1	49.33	49.33	58.92	47.95	50	49.33	44.64	50	46.42	44.64	75	58.92
s2	82.14	74.67	91.07	82.14	92.85	88.47	94.64	92.85	100	92.85	100	92.85
s3	49.95	51.58	47.95	47.95	47.44	49.95	53.06	49.86	60.71	53.86	59.18	54.95
s4	62.33	64.66	73.66	71.22	66.07	56.83	69.64	64.66	85.71	69.64	88.39	82.36
s5	46.42	46.42	48.41	47.66	51.58	50.14	46.42	48.95	63.09	51.86	82.14	71.86

TABLE 1: Obtained classification accuracy (%) for different E2ZTW parameters

$s \in S$	TP(%)	FN(%)	FP(%)	TN(%)	Pr(%)	$NPv(\%)$	$S_e(\%)$	$S_p(\%)$
s1	48.6	1.4	11.1	38.9	81.4	96.6	77.8	97.2
s2	35.42	14.58	9.7	40.3	78.46	72.5	70.83	69.4
s3	43.8	6.3	0.0	50	100	88.9	100	87.5
s4	9	41	0.7	49.3	92.9	54.6	98.6	18.1
s5	30.55	19.4	7.63	42.36	78.43	65.53	84.72	61.1
s6	31.94	18.05	10.41	39.58	75.40	70.37	79.16	63.88
s7	45.1	4.9	9.7	40.3	82.3	89.2	80.6	90.3
s8	48.6	1.4	2.08	47.91	95.89	97.18	95.83	97.2
s9	40.97	9.02	2.08	47.91	95.2	84.1	95.8	81.9
s1	48.88	1.11	1.11	48.88	97.77	97.77	97.77	97.77
s2	34.44	15.55	11.11	38.89	75.60	71.42	77.77	68.88
s3	45.55	4.44	2.22	47.78	95.34	91.48	95.55	91.11
s1	41.1	12.5	12.5	33.9	76.7	73.1	73.1	76.7
s2	50	0.0	50	0.0	100	100	100	100
s3	35.71	14.28	26.53	23.46	56.45	62.16	46.93	71.42
s4	47.8	1.3	10.26	40.62	82.30	96.80	79.82	97.27
s5	36.9	11.50	5.95	28.98	86.11	79.86	88.46	76.22

(a) Statistical testing of the proposed approach

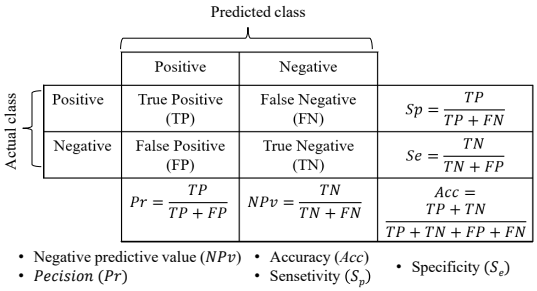

(b) Confusion matrix labels

TABLE 2: Detailed results of the proposed method

systems, which are based on tracking continuously the brain rhythmic activities. The proposed signal processing chain outperforms those of previous studies, e.g., the average accuracy herein is increased by 17% compared to the method presented in [34]. Furthermore, the proposed approach outperforms systems based on SVM classifier with CSP and with the filter bank common spatial pattern (FBCSP). Indeed, the average accuracy is increased by 7% and 3% respectively [29], [35]. Moreover, the proposed approach improves the runtime by reducing the number of studied samples and channels while ensuring good accuracy, contrary to the method presented in [29]. For example, in [29], average classification accuracy is achieved through the use of different feature extraction and classification algorithms, which are known to increase runtime. Moreover, contrary to other methods presented in [29], [36]–[38] the proposed approach improves the runtime by reducing the number of studied samples and channels while ensuring a high accuracy. In fact, the proposed approach allows to localize the EEG epoch while optimizing the length of the frame window as much as possible instead of using a fixing starting time point of MI and a fixing epoch duration as in the case of the study presented in [29]; which has used a fixed frame window of 2s. Using the same dataset and compared to the presented system in [29], the proposed approach shows that the optimal frame window length is 1.5s which means that the system processes during the training and testing phases $\frac{Fs}{2}$ irrelevant samples. Furthermore, the proposed approach reduces the number of

This work is licensed under a Creative Commons Attribution 4.0 License. For more information, see https://creativecommons.org/licenses/by/4.0/.

This article has been accepted for publication in a future issue of this journal, but has not been fully edited. Content may change prior to final publication. Citation information: DOI 10.1109/ACCESS.2020.3017888, IEEE Access

$s \in S$	Proposed method	[29]	[9]	[10]	[12]	[33]	[34]	[35]
s1	87.50	88.88	88.89	86.81	91.67	90.21	91.61	81
s2	75.69	80.55	54.86	63.89	59.72	63.28	57.03	54.37
s3	93.75	93.05	96.53	94.44	95.83	96.55	90.21	50.87
s4	58.3	52.09	70.14	68.75	77.08	76.38	73.61	98.75
s5	72.91	87.5	65.97	56.25	67.36	65.49	73.94	71.5
s6	71.52	90.27	61.81	69.44	69.44	69.01	68.31	75.62
s7	85.41	92.36	81.25	78.47	78.47	81.94	75	84.50
s8	96.52	85.41	95.83	97.91	97.22	95.14	95.14	81.12
s9	88.88	92.36	90.97	93.75	88.19	93.01	90.21	79.12
s1	97.77	100	98.89	97.77	86.6	100	96.66	NA
s2	73.33	61.66	71.67	61.66	78	76.67	60	NA
s3	93.33	93.33	93.33	93.33	56	100	88.33	NA
s1	75	69.64	69.64	66.79	N/A	58	22	82.86
s2	100	96.42	98.21	96.07	N/A	10	86	98.71
s3	59.18	60.57	54.59	52.14	N/A	47	25	69.64
s4	88.39	70.53	71.88	71.43	N/A	79	13	93.50
s5	82.14	78.57	85.32	50	N/A	77	0	94.93
Mean	82.32	81.95	79.4	76.40	78.79	77.56	65.06	79.74
Std	13.02	14.18	15.3	16.99	13.65	23.44	31.23	14.78

TABLE 3: Classification accuracy (%) (Mean and Standard deviation in percent) of the proposed approach and other MI classification approaches on each subject.

channels because signals from some channels containing redundant information, noise and artefacts as the case of the E_{OG} channels used during the recording process. So, the proposed approach identified and selected the channels that are containing correlated and relevant information in the trials T of the training and testing datasets.

The high-resolution properties of the numerator of the group delay were successfully used to localize the SMRs for the left- and right-hand movement. It is worthy of note that the SMRs can be seen when the trial segment (i.e., time window size) is less than 25 ms. The resulting spectral features can be derived at every sampling instant, and hence, the E2ZTW method provides instantaneous spectrum analysis. It has been shown that spectral information is strongest for epochs near the moments when a subject is thinking. This spectral information can be well localized using the proposed analysis method. Furthermore, the E2ZTW approach can be used to identify EEG channels that have useful information and trials that contain only artifacts without the presence of any sensorimotor rhythmic activity. The high-resolution properties of the proposed approach may help in pathological disorder analysis, such as autism or epilepsy, where brain activities need to monitored (track) continuously and in real-time to predict certain events.

V. CONCLUSION

This paper presented a new MI-based BCI analysis approach. The approach is based on the concept of E2ZTW and allows the dynamic tracking of the SMRs in the brain, related to the right- and left-hand movements. The approach also allows the preprocessing of spectral information through successive integration of frequency domain samples. The high temporal resolution provided by the E2ZTW analysis allows the extraction of spectral features related to SMR from trials without any prior information about the trigger or the cue pointed to the start of MI tasks. Thus, the proposed method selects the temporal regions containing the relevant information and recognizes the trials containing artifacts without recourse to the feedbacks provided by an expert. It is worth noting that the proposed method allows, at the same time, the selection of the relevant channels containing SMRs. The proposed approach has been successful in recognizing the EEG channels used during the recording process without any prior information on the trials containing artifacts identified by the expert. We have shown that the system accuracy can be significantly increased by integrating the E2ZTW approach into it, which increases the system accuracy by more than 20% for some subjects. Moreover, the integration of the proposed method into the system significantly improves the runtime of the EEG signal processing chain due to a significant reduction of the number of both temporal samples and EEG channels.

ACKNOWLEDGMENT

The authors extend their appreciation to the Deanship of Scientific Research at King Saud University for funding this work through Research Group no. RG-1440-109.

REFERENCES

[1] B. A. Cociu, S. Das, L. Billeci, W. Jamal, K. Maharatna, S. Calderoni, A. Narzisi, and F. Muratori, "Multimodal functional and structural brain connectivity analysis in autism: A preliminary integrated approach with EEG, fMRI, and DTI," IEEE Transactions on Cognitive and Developmental Systems, vol. 10, pp. 213–226, June 2018.

[2] S. Jacob, M. Alagirisamy, V. G. Menon, B. M. Kumar, N. Z. Jhanjhi, V. Ponnusamy, P. G. Shynu, and V. Balasubramanian, "An adaptive and flexible brain energized full body exoskeleton with IoT edge for assisting the paralyzed patients," IEEE Access, vol. 8, pp. 100721–100731, 2020.

[3] J. Li, C. Li, and A. Cichocki, "Canonical polyadic decomposition with auxiliary information for brain–computer interface," IEEE Journal of Biomedical and Health Informatics, vol. 21, pp. 263–271, Jan. 2017.

[4] P. Autthasan, X. Du, J. Arnin, S. Lamyai, M. Perera, S. Itthipuripat, T. Yagi, P. Manoonpong, and T. Wilaiprasitporn, "A single-channel consumer-grade EEG device for brain–computer interface: Enhancing detection of SSVEP and its amplitude modulation," IEEE Sensors Journal, vol. 20, pp. 3366–3378, Mar. 2020.

[5] A. Ditthapron, N. Banluesombatkul, S. Ketrat, E. Chuangsuwanich, and T. Wilaiprasitporn, "Universal joint feature extraction for p300 EEG classification using multi-task autoencoder," IEEE Access, vol. 7, pp. 68415–68428, 2019.

[6] G. Pfurtscheller and F. L. Da Silva, "Event-related eeg/meg synchronization and desynchronization: basic principles," Clinical neurophysiology, vol. 110, no. 11, pp. 1842–1857, 1999.

[7] P. Sawangjai, S. Hompoonsup, P. Leelaarporn, S. Kongwudhikunakorn, and T. Wilaiprasitporn, "Consumer grade EEG measuring sensors as research tools: A review," IEEE Sensors Journal, vol. 20, pp. 3996–4024, Apr. 2020.

[8] T.-E. Kam, H.-I. Suk, and S.-W. Lee, "Non-homogeneous spatial filter optimization for electroencephalogram EEG-based motor imagery classification," Neurocomputing, vol. 108, no. 0, pp. 58 – 68, 2013.

[9] F. Lotte and C. Guan, "Regularizing common spatial patterns to improve bci designs: Unified theory and new algorithms," IEEE Transactions on Biomedical Engineering, vol. 58, no. 2, pp. 355–362, 2011.

[10] K. Belwafi, O. Romain, S. Gannouni, F. Ghaffari, R. Djemal, and B. Ouni, "An embedded implementation based on adaptive filter bank for brain–computer interface systems," Journal of Neuroscience Methods, vol. 305, pp. 1–16, July 2018.

[11] B. Blankertz, R. Tomioka, S. Lemm, M. Kawanabe, and K. Muller, "Optimizing spatial filters for robust eeg single-trial analysis," IEEE Signal Processing Magazine, vol. 25, no. 1, pp. 41–56, 2008.

[12] A. Malekmohammadi, H. Mohammadzade, A. Chamanzar, M. Shabany, and B. Ghojogh, "An efficient hardware implementation for a motor imagery brain computer interface system," Scientia Iranica, vol. 0, pp. 0–0, Aug. 2018.

This work is licensed under a Creative Commons Attribution 4.0 License. For more information, see https://creativecommons.org/licenses/by/4.0/.

This article has been accepted for publication in a future issue of this journal, but has not been fully edited. Content may change prior to final publication. Citation information: DOI 10.1109/ACCESS.2020.3017888, IEEE Access

[13] Z. Y. Chin, K. K. Ang, C. Wang, C. Guan, and H. Zhang, "Multi-class filter bank common spatial pattern for four-class motor imagery bci," in Engineering in Medicine and Biology Society, 2009. EMBC 2009. Annual International Conference of the IEEE, pp. 571–574, Sept 2009.

[14] J. Feng, E. Yin, J. Jin, R. Saab, I. Daly, X. Wang, D. Hu, and A. Cichocki, "Towards correlation-based time window selection method for motor imagery BCIs," Neural Networks, vol. 102, pp. 87–95, June 2018.

[15] D. L. Schomer and F. H. L. da Silva, eds., Niedermeyer's Electroencephalography: basic principles, clinical applications, and related fields. Oxford University Press, Nov. 2017.

[16] K. P. Thomas, C. Guan, C. T. Lau, A. P. Vinod, and K. K. Ang, "A new discriminative common spatial pattern method for motor imagery brain 2013;computer interfaces," IEEE Transactions on Biomedical Engineering, vol. 56, pp. 2730–2733, Nov 2009.

[17] J. Meng, J. H. Mundahl, T. D. Streitz, K. Maile, N. S. Gulachek, J. He, and B. He, "Effects of soft drinks on resting state EEG and brain–computer interface performance," IEEE Access, vol. 5, pp. 18756–18764, 2017.

[18] A. Schlögl, F. Lee, H. Bischof, and G. Pfurtscheller, "Characterization of four-class motor imagery EEG data for the BCI-competition 2005," Journal of neural engineering, vol. 2, no. 4, p. L14, 2005.

[19] D. L. Schomer and F. L. Da Silva, Niedermeyer's electroencephalography: basic principles, clinical applications, and related fields. Lippincott Williams and Wilkins, 2012.

[20] J. Jin, Y. Miao, I. Daly, C. Zuo, D. Hu, and A. Cichocki, "Correlation-based channel selection and regularized feature optimization for MI-based BCI," Neural Networks, vol. 118, pp. 262–270, Oct. 2019.

[21] P. Cheng, P. Autthasan, B. Pijarana, E. Chuangsuwanich, and T. Wilaiprasitporn, "Towards asynchronous motor imagery-based brain-computer interfaces: a joint training scheme using deep learning," in TENCON 2018 - 2018 IEEE Region 10 Conference, IEEE, Oct. 2018.

[22] R. Chaisaen, P. Autthasan, N. Mingchinda, P. Leelaarporn, N. Kunaseth, S. Tammajarung, P. Manoonpong, S. C. Mukhopadhyay, and T. Wilaiprasitporn, "Decoding EEG rhythms during action observation, motor imagery, and execution for standing and sitting," IEEE Sensors Journal, pp. 1–1, 2020.

[23] G. Dornhege, B. Blankertz, G. Curio, and K.-R. Muller, "Boosting bit rates in noninvasive EEG single-trial classifications by feature combination and multiclass paradigms," IEEE Transactions on Biomedical Engineering, vol. 51, pp. 993–1002, June 2004.

[24] A. Schlögl, F. Lee, H. Bischof, and G. Pfurtscheller, "Characterization of four-class motor imagery EEG data for the BCI-competition 2005," Journal of Neural Engineering, vol. 2, pp. L14–L22, aug 2005.

[25] M. Naeem, C. Brunner, R. Leeb, B. Graimann, and G. Pfurtscheller, "A seperability of four-class motor imagery data using independent components," Journal of neural engineering vol. 10, pp. 208–216, 2006.

[26] K. S. R. Murty and B. Yegnanarayana, "Epoch extraction from speech signals," IEEE Transactions on Audio, Speech, and Language Processing, vol. 16, pp. 1602–1613, Nov 2008.

[27] K. S. R. Murty and B. Yegnanarayana, "Epoch extraction from speech signals," IEEE Transactions on Audio, Speech, and Language Processing, vol. 16, pp. 1602–1613, Nov. 2008.

[28] G. Pfurtscheller, "Functional brain imaging based on ERD/ERS," Vision Research, vol. 41, pp. 1257–1260, May 2001.

[29] K. Belwafi, S. Gannouni, H. Aboalsamh, H. Mathkour, and A. Belghith, "A dynamic and self-adaptive classification algorithm for motor imagery EEG signals," Journal of Neuroscience Methods, vol. 327, p. 108346, Nov. 2019.

[30] F. Lotte, M. Congedo, A. Lécuyer, F. Lamarche, and B. Arnaldi, "A review of classification algorithms for eeg-based brain-computer interfaces," Journal of Neural Engineering, vol. 4, no. 2, p. R1, 2007.

[31] S. Taheri and M. Ezoji, "EEG-based motor imagery classification through transfer learning of the CNN," in 2020 International Conference on Machine Vision and Image Processing (MVIP), IEEE, Feb. 2020.

[32] F. Lotte, M. Congedo, A. Lecuyer, F. Lamarche, and B. Arnaldi, "A review of classification algorithms for EEG-based brain computer interfaces," Journal of Neural Engineering, vol. 4, no. 2, p. R1, 2007.

[33] A. Singh, S. Lal, and H. Guesgen, "Reduce calibration time in motor imagery using spatially regularized symmetric positives-definite matrices based classification," Sensors, vol. 19, p. 379, Jan. 2019.

[34] A. Barachant, S. Bonnet, M. Congedo, and C. Jutten, "Multiclass brain–computer interface classification by riemannian geometry," IEEE Transactions on Biomedical Engineering, vol. 59, pp. 920–928, Apr. 2012.

[35] S. Kumar, A. Sharma, and T. Tsunoda, "An improved discriminative filter bank selection approach for motor imagery EEG signal classification using mutual information," BMC Bioinformatics, vol. 18, Dec. 2017.

[36] T. Jia, K. Liu, Y. Lu, Y. Liu, C. Li, L. Ji, and C. Qian, "Small-dimension feature matrix construction method for decoding repetitive finger movements from electroencephalogram signals," IEEE Access, vol. 8, pp. 56060–56071, 2020.

[37] Z. Tayeb, J. Fedjaev, N. Ghaboosi, C. Richter, L. Everding, X. Qu, Y. Wu, G. Cheng, and J. Conradt, "Validating deep neural networks for online decoding of motor imagery movements from EEG signals," Sensors, vol. 19, p. 210, Jan. 2019.

[38] F. Lotte and C. Guan, "Regularizing common spatial patterns to improve BCI designs: Unified theory and new algorithms," Biomedical Engineering, IEEE Transactions on vol. 58, pp. 355–362, Feb 2011.

KAIS BELWAFI was born in Mezzouna, Sidi Bouzid, Tunisia in 1985. He received his PhD degree in sciences and technologies of information and communication technology from the University of Cergy Pontoise, France, in 2017. He received his Master degree in smart and communication systems from the highest school of engineering of Sousse, Tunisia, in 2012. Currently, he is researcher at the College of Computer and Information Sciences, King Saud University. His main areas of research include human computer interface, machine learning, signal processing, embedded and real-time systems, HW/SW co-design, etc.

SOFIEN GANNOUNI received his master's degree in computer science from Paul Sabatier University (Toulouse III - France), and his PhD degree in Computer Science from Pierre & Marie Curie University (Paris VI - France). Currently, he is Associate Professor at College of Computer and Information Sciences, King Saud University. His main research interests include Brain Computer Interfaces, Computational Intelligence, Machine learning, and High-Performance Computing.

HATIM ABOALSAMH received his PhD degree in computer engineering and science from the University of Miami, USA, in 1987. He is currently a Professor and the Chairman with the Department of Computer Science, King Saud University (KSA), Riyadh, Saudi Arabia. He was the Vice Rector for Development and Quality, KSA, from 2006 to 2009, and the Dean of the College of Computer and Information Sciences. His research interests include pattern recognition, biometrics, probability modeling, and machine learning. He is a Fellow Member of the British Computer Society, and a Senior Member of the Association of Computing Machinery, USA, and the International Association of Computer Science and Information Technology. He was the Vice President of the Saudi Computer Society. He was the Editor in-Chief of the KSU-Journal of Computer Sciences. He is currently the Editor-in-Chief of the Applied Computing and Informatics Journal (Elsevier) and of the Saudi Computer Society Journal.

This work is licensed under a Creative Commons Attribution 4.0 License. For more information, see https://creativecommons.org/licenses/by/4.0/.